Chemistry International 7(2) (2021) 90-102

International Scientific Organization
http://iscientific.org/
Chemistry International
www.bosaljournals.com/chemint/

$Fe(OH)_3$/kaolinite nanoplatelets: Equilibrium and thermodynamic studies for the adsorption of Pb(II) ions from aqueous solution

Akl M. Awwad*[1], Maisa'a W. Shammout[2] and Mohammad W. Amer[3]

[1]Department of Nanotechnology, Royal Scientific Society, Amman, Jordan
[2]Water, Energy and Environment Center, The University of Jordan, Amman, Jordan
[3]Department of Chemistry, Faculty of Science, The University of Jordan, Amman, Jordan
*Corresponding author's E. mail: akl.awwad@yahoo.com

A R T I C L E I N F O

Article type:
Research article
Article history:
Received July 2020
Accepted December 2021
April 2021 Issue
Keywords:
Kaolin clay
$Fe(OH)_3$/kaolinite nanoplatelets
Adsorption
Pb(II) ions
Thermodynamics

A B S T R A C T

Development of a sustainable route for preparation $Fe(OH)_3$/kaolinite nanoplatelets from Batin El-Ghoul clay deposits, south Jordan with uniform plate-like morphology. $Fe(OH)_3$/kaolinite nanoplatelets is an efficient adsorbent for the removal of Pb(II) ions from aqueous solutions. Effects of pH solution, adsorbent dose, initial metal ion concentration, contact time, and temperature on the adsorption process were examined. The Langmuir isotherm model is the best fit model to predict the experimental data and the adsorption capacity. Maximum adsorption capacity on Langmuir isotherm was 370.37 mg/g. Thermodynamic parameters revealed that the negative values of ΔG^o and the positive value of ΔH^o, the adsorption process was spontaneous and endothermic. Results revealed that $Fe(OH)_3$/kaolinite is promising for the removal of metal ions from effluents.

Capsule Summary: $Fe(OH)_3$/kaolinite nanoplatelets with defined surface and physicochemical properties were developed and employed for the removal Pb(II) ions. $Fe(OH)_3$/kaolinite showed maximum adsorption capacity of 370.37 mg/g and have potential for the remediation of wastewater contains heavy metal ions.

Cite This Article As: A. M. Awwad, M. W. Shammout and M. W. Amer. $Fe(OH)_3$/kaolinite nanoplatelets: Equilibrium and thermodynamic studies for the adsorption of Pb(II) ions from aqueous solution. Chemistry International 7(2) (2021) 90-102. https://doi.org/10.5281/zenodo.4442351

INTRODUCTION

Pb(II) ions are toxic trace elements occurring in natural water, aqueous solutions and industrial wastewater. The maximum permissible limit (mg/L) for Pb(II) ions in water is 0.05 mg/L (World Health Organization, WHO). In industrial wastewaters, lead ions concentration approach 100–400 mg/L; this concentration is very high in relation to water quality standards, and lead ion concentration of wastewaters must be reduced to a level of 0.05–0.10 mg/L before discharging to water ways or sewage systems (United States Environmental Protection Agency, USEPA). Many processes have been developed for removal of Pb(II) ions from water, aqueous solutions and industrial wastewater such as precipitation, coagulation-flocuulation, ion exchange, cementation, electro dialysis, electro winning, electro coagulation and reverse osmosis (Mansoorian et al. 2014; .Al-shannay et al., 2015; Eiband et al. 2014; Kavak, 2013; Lin and Xu, 2014; Pang et al., 2011). Recently scientific researchers concentrated their research work on using agricultural wastes through biosorption processes for the removal of Pb(II) ions from aqueous and industrial wastewater by phoenix tree leaves (Liang et al., 2016), rice husk ash (Feng et

al., 2004), peanut husk (Abdelfattah et al., 2016), *Militia ferruginea* plant leaves (Mengistie et al., 2008), pine cone activated carbon (Momčilović et al., 2011), lentil husk (Basu et el., 2015), modified soda lignin (MSL) extracted from oil palm empty fruit bunches (Ibrahim et al., 2010), olive stone waste (Fiol et al., 2006), durian tree sawdust, coconut coir and oil palm empty fruit bunch (Yusoff et al., 2014), *Moringa oleifera* bark (Reddy et al., 2010), sulfured orange peel (Liang et al., 2016), *Acacia leucocephala* bark powder (Munagapati et al., 2019). Natural materials used as adsorbents for the removal of Pb(II) ions from water, aqueous solutions and industrial wastewater are reported in the open literature such as natural bentonite (Esmaeili et al., 2019), natural sepiolite (Bektas et al., 2004), kaolinite/smectite natural composite adsorbent (El-Naggar et al., 2019), natural diatomite (Brlgin and Tulun, 2015; El sayed, 2018), raw clay and broken clay brick waste (El-Shahat et al., 2014), kaolinite clay (Omar et al., 2007; Al-Jalil and Alsewailem, 2009), polyphosphate modified kaolinite clay (Amer et al., 2010; Unuabonah et al., 2007), modified with aluminium sulfate and unmodified kaolinite clay (Jiang et al., 2009), natural kaolinite clay (Jiang et al., 2010), calcined corncob-kaolinite (Chukwuemeka-Okorie et al., 2018), natural mixture of kaolinite-albite-montmorillonite-illite clay (Eba et al., 2011), natural zeolite (Erdem et al., 2004) and activated bentonite (Kul et al., 2010).

Emerging nanotechnology has been gaining increasing interest and many nanomaterials have been developed to remove heavy metals from polluted water, due to their excellent features resulting from the nanoplatelets structure. Novel nonmaterial for removal Pb(II) ions from water and industrial wastewater as reported in literature such as hydroxyapatite nanomaterial (Mousa et al., 2016), cadmium sulfide nanoparticles (Golkhah et al., 2017), nanocarbon materials, nanometal particles, and polymer-supported nanoparticles (Wang et al., 2012), low-temperature exfoliated graphene nanosheets (Huang et al., 2011), graphene oxide-$MnFe_2O_4$ magnetic nanohybrids (Kumar et al., 2014), alumina-coated carbon nanotubes (Gupta et al., 2011), a functionalized single-walled carbon nanotube (Anitha et al., 2015), multiwalled carbon nanotubes (Li et al., 2003), carbon nanotubes (Li et al., 2002), acidified carbon nanotubes (Wang et al., 2007), manganese oxide-coated carbon nanotubes (Wang et al., 2007), functionalized multi-walled carbon nanotube with both amino and thiolated groups (Hadavifar et al., 2014), nanoIllite/smectite clay (Yin et al., 2018), carbon-based nanomaterials, zero-valent metal, metal-oxide based nanomaterials, and nanocomposites (Yang et al., 2019), superparamagnetic monodispersed iron oxide (Fe_3O_4) nanoparticles (Sarkar and Sarkar, 2013), purified and polyhydroxylbutyrate functionalized carbon nanotubes adsorbents (Bankole et al., 2019).

This research work was concentrated on using $Fe(OH)_3$/kaolinite nanoplatelets extracted from the Jordanian kaolin clay as high efficient adsorbent for Pb(II) ions from aqueous solutions. The prepared $Fe(OH)_3$/kaolinite nanoplatelets showed a high adsorption capacity for Pb(II) ions in aqueous solution.

MATERIAL AND METHODS

Chemical and reagents

Hydrochloric acid (HCL, 37%) and lead acetate dihydrate $Pb(CH_3COO)_2.2H_2O$ were purchased from Merck, Germany. Kaolin clay was obtained from Batn El-Ghul deposits, south Jordan. Distilled and de-ionized water from our laboratory were used in all our experimental work.

Preparation of nanoplatelets $Fe(OH)_3$/kaolinite

First of all, the samples of kaolin clay were washed with de-ionized water to remove organic materials and water soluble metal ions and then by decantation and drying at 80°C for 4h. 1Kg of kaolin clay dried powder was treated with 500ml diluted hydrochloric acid (10-20%) with stirring from time to time during 6h. An emulsion was formed consisted mainly from kaolinite clay, iron, potassium, sodium, magnesium, calcium salts and traces of titanium oxide. The brown-white emulsion was treated with sodium hydroxide (10% NaOH) solution drop wise under magnetic stirring for 2h, until the emulsion changed from acidic to alkaline. The obtained emulsion was filtered on Whatmans filter paper No. 1 at laboratory temperature (27°C). Afterwards, the obtained mixture of iron hydroxide and kaolinite clay was subjected to centrifuging, washing and drying in an electric oven at 80°C for 4h to obtain very fine brown-white powder. This powder was subjected for analysis by XRF, XRD, FT-IR, SEM and TEM.

Batch adsorption procedure

Stock solutions of Pb(II) were prepared by dissolving appropriate amounts of $Pb(CH_3COO)_2{\cdot}2H_2O$ in de-ionized water. Batch adsorption experiments were carried out in a series of conical flasks by mixing a constant amount of nano $Fe(OH)_3$/kaolinite and 100mL of the aqueous solution of Pb(II) ions at varying concentration and different temperatures. Then, the conical flasks were put in a shaker incubator at 150 rpm for a certain time interval, the $Fe(OH)_3$/kaolinite nanoplatelets was separated from the aqueous solutions by centrifugation at 3000 rpm for 5 min, and the supernatant was subjected to filtration through a Whitman filter paper No. 2. Pb(II) concentration in the solutions was measured by AAS600 atomic spectrophotometer. The percent removal (R) and adsorption capacity (q_e) of Pb(II) ions onto $Fe(OH)_3$/kaolinite nanoplatelets in the batch test was calculated using the equations:

$$R\ (\%) = \frac{C_o - C_e}{C_o} \text{ x } 100 \qquad (1)$$

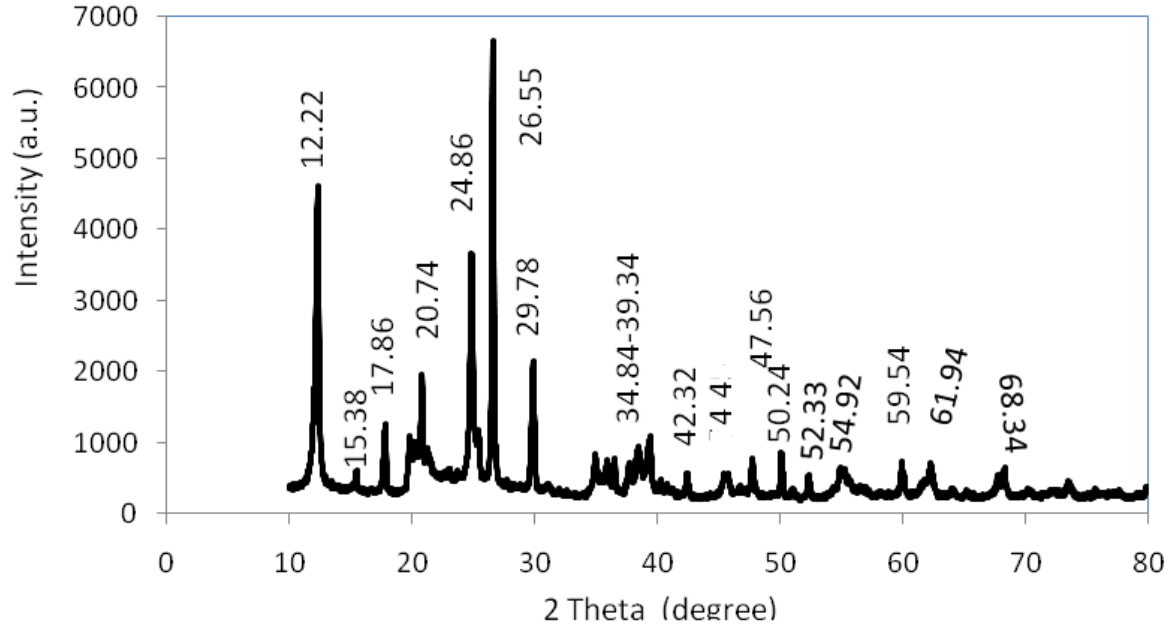

Fig. 1: XRD of raw Jordanian kaolin clay

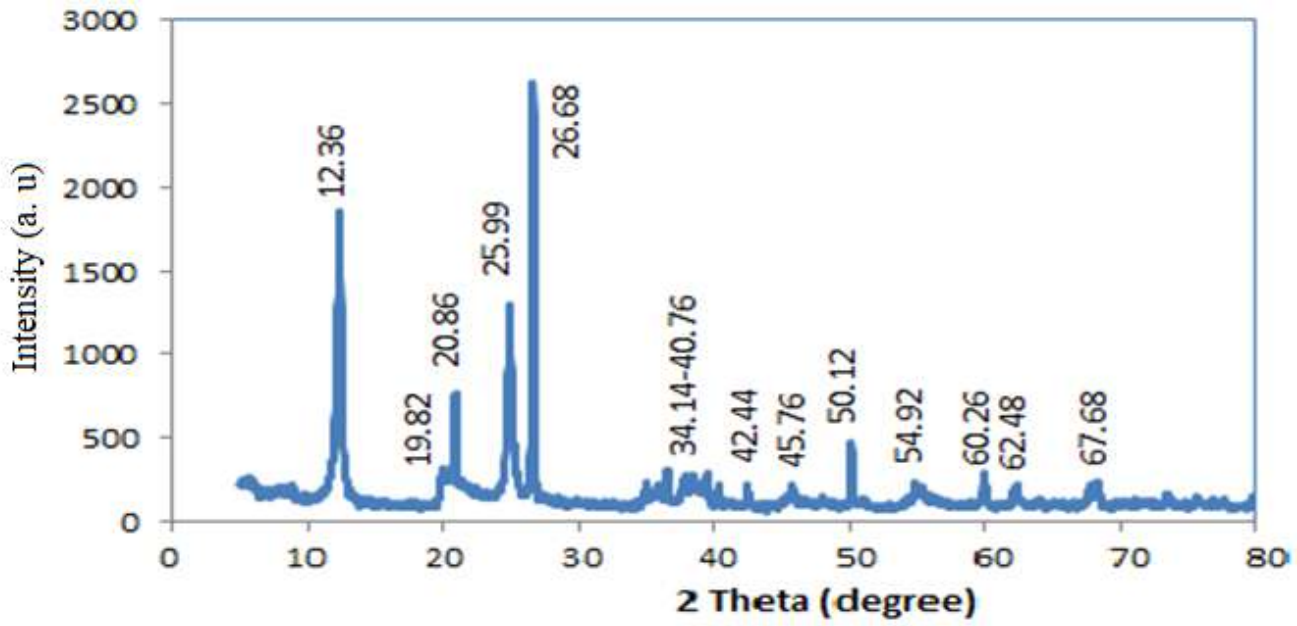

Fig. 2: XRD of $Fe(OH)_3$/kaolinite nanoplatelets

$$q_e = \frac{C_o - C_e}{M} \; x \; V \qquad (2)$$

Where, %R is the Pb(II) ions removal percent, q_e is the equilibrium capacity of lead onto the nano $Fe(OH)_3$/kaolinite, C_o is the initial concentration of the Pb(II) solution, mg/L, C_e is the equilibrium concentration of the Pb(II) solution, mg/L. V (L) is the volume of the solution and M (g) is the mass of $Fe(OH)_3$/kaolinite nanoplatelets. All assays were carried out in triplicate and only mean values are presented.

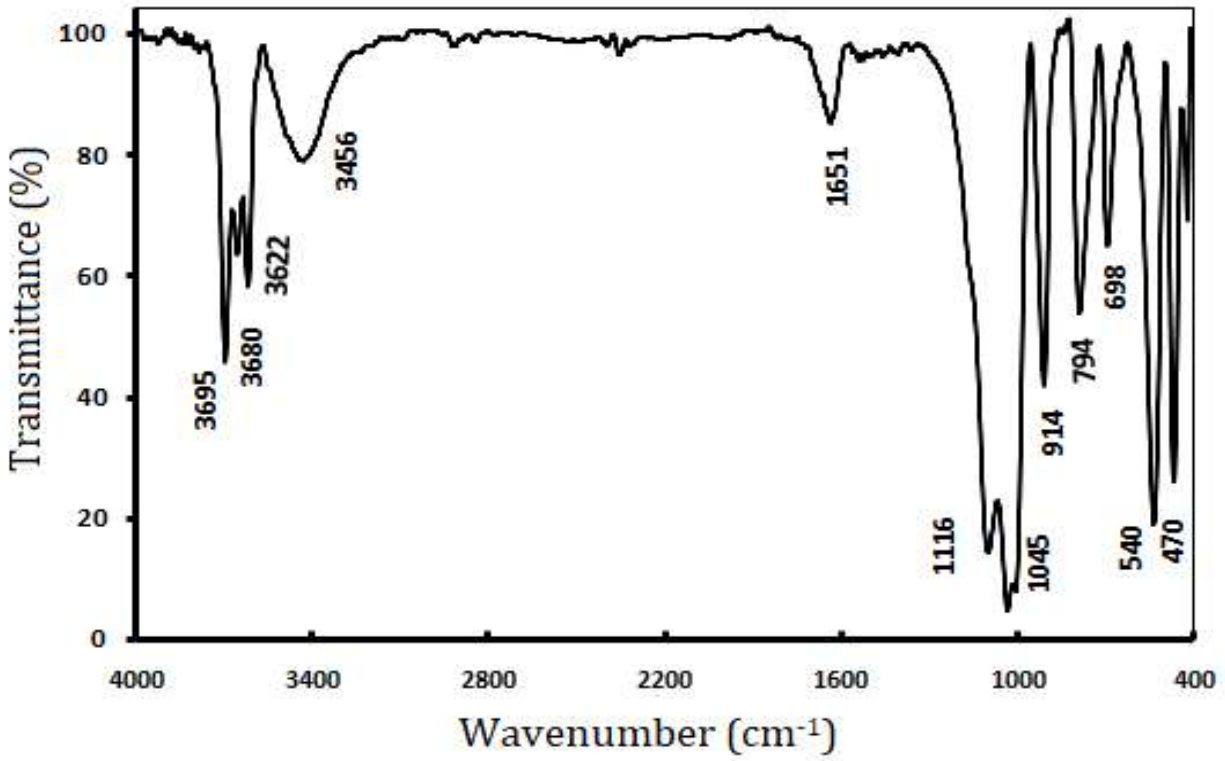

Fig. 3: FT-IR of raw Jordanian kaolin clay

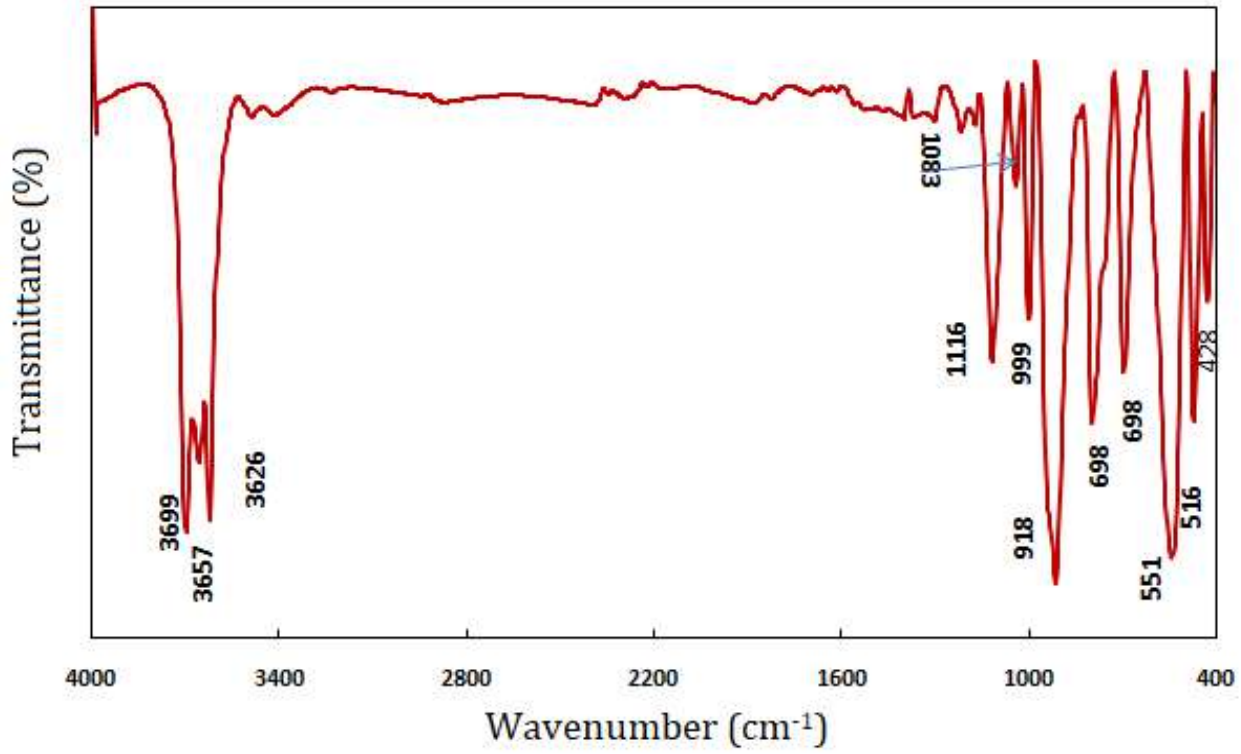

Fig. 4: FT-IR of $Fe(OH)_3$/kaolinite nanoplatelets

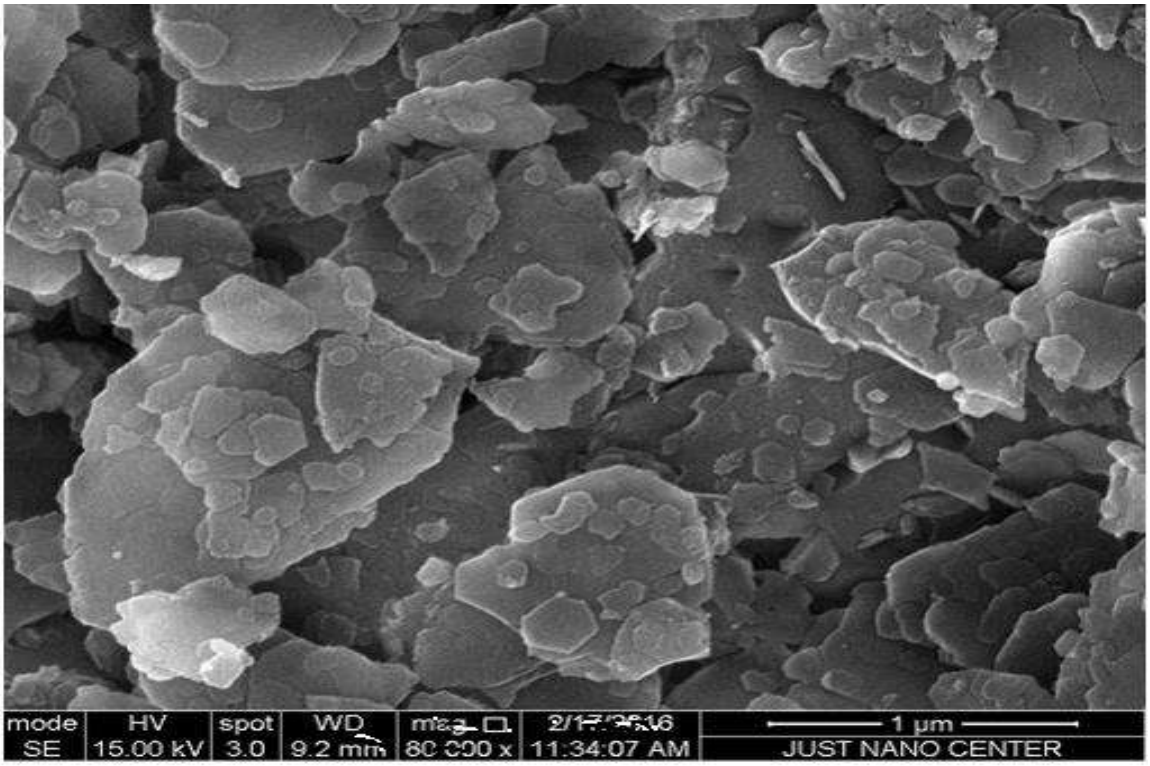

Fig. 5: Scanning electron microscopy (SEM) image of raw Jordanian kaolin clay

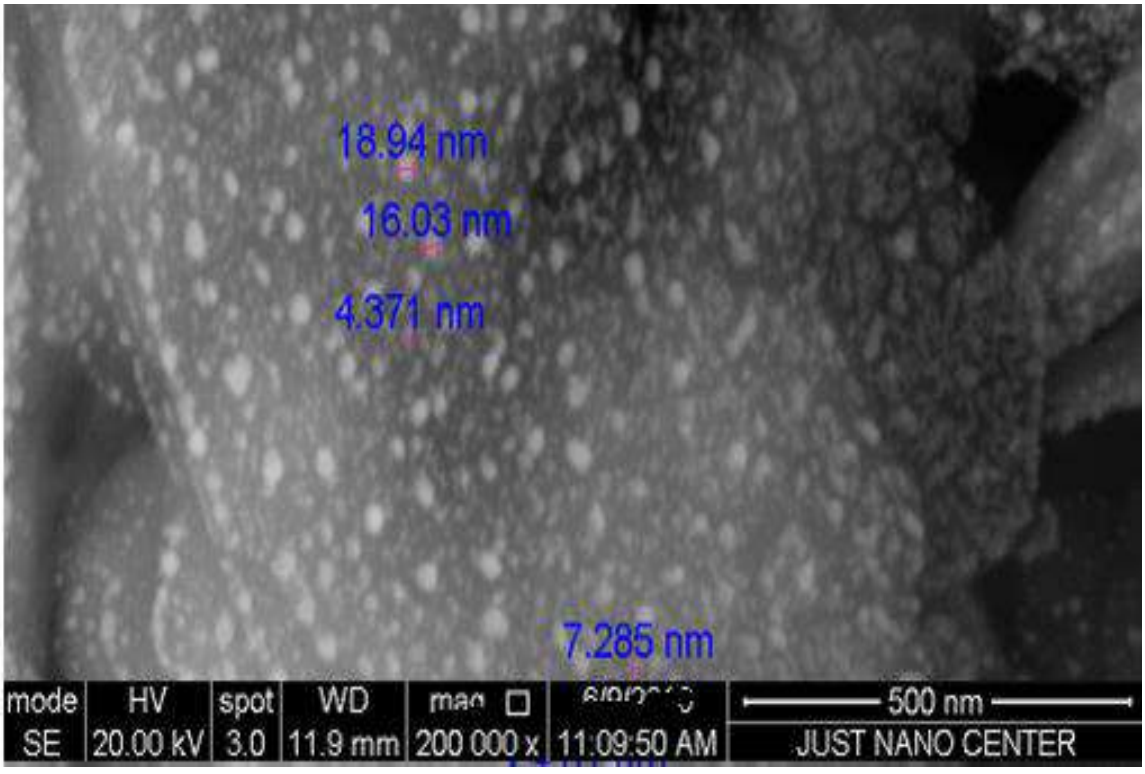

Fig. 6: Scanning electron microscopy (SEM) of the prepared $Fe(OH)_3$/kaolinite nanoplatelets

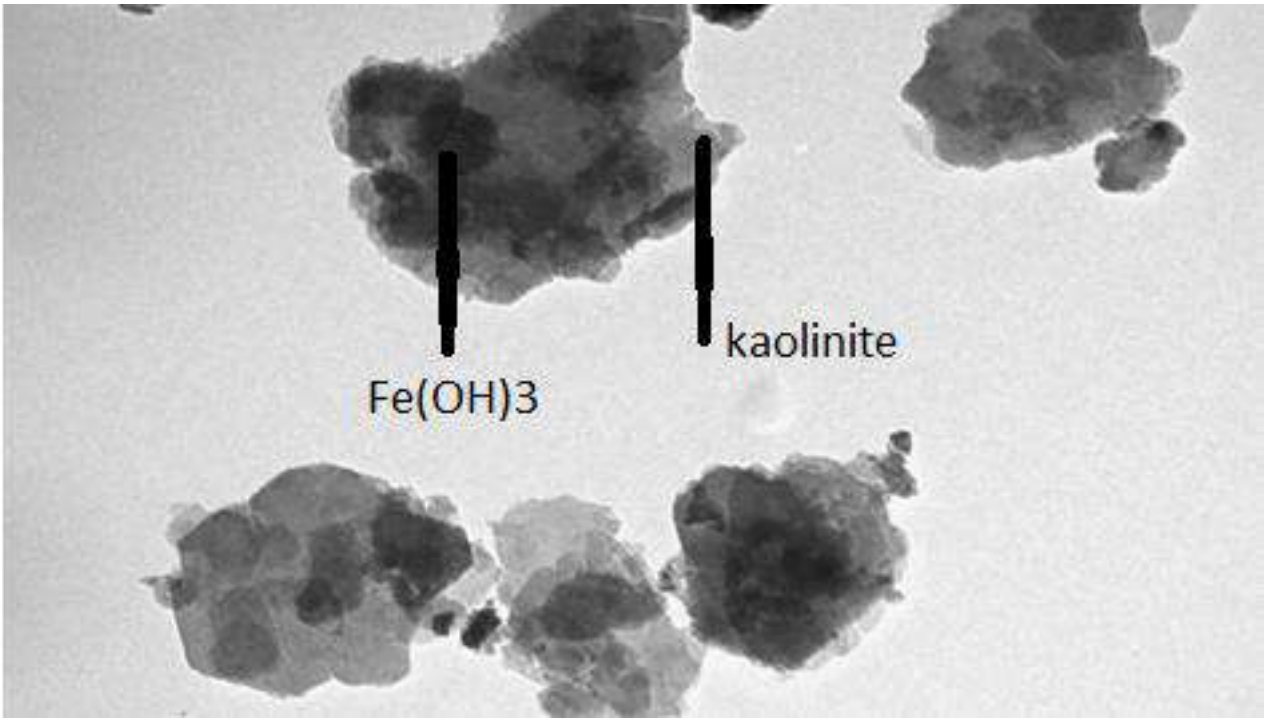

Fig. 7: Transmission electron microscope (TEM) of the prepared nano $Fe(OH)_3$/kaolinite from the raw Jordanian kaolin clay

Characterization techniques

The Fourier transform infrared (FT-IR) spectra of nano $Fe(OH)_3$/kaolinite were recorded with the Fourier transform infrared spectrophotometer (IR-Prestige 21 spectrophotometer, Shimadzu). X-ray diffraction (XRD) analysis was determined by X-ray diffract meter (XRD-6000, Shimadzu). The morphology of nano $Fe(OH)_3$/kaolinite was analyzed by a scanning electron microscope (SEM, Hitachi S4700) and transmission electron microscope (TEM, Hitachi HF5000), Pb(II) ons concentration was determined by atomic spectrophotometer (AAS600, Shimadzu, Japan) and pH measurements were made with a WTW PH meter using combined glass electrode.

RESULTS AND DISCUSSION

XRF and XRD analysis

Raw kaolin clay obtained from Batin El Ghoul, south Jordan and the prepared $Fe(OH)_3$/kaolinite nanoplatelets were analyzed by X-ray fluorescence (XRF). The chemical composition of raw Jordanian kaolin clay determined as: 60.23% SiO_2, 18.94% Al_2O_3, 8.76% Fe_2O_3, 1.04% TiO_2, 0.54% CaO, 0.42% MgO, 0.02% Na_2O, 1.22% K_2O and 7.78% loss of ignition. The prepared $Fe(OH)_3$/kaolinite nanocomposite analysis as: 74.61% SiO_2, 17.82% Al_2O_3 and 7.23% $Fe(OH)_3$. XRF analysis showed that the ratio of SiO_2/Al_2O_3 equals 3.18 for raw kaolin clay and 4.19 for the prepared $Fe(OH)_3$/kaolinite nanocomposite. Figure 1 showed the X-ray diffraction (XRD) of raw Jordanian kaolin clay and Figure 2 the XRD of $Fe(OH)_3$/kaolinite nanoplatelets, indicating the removal of associated minerals with raw kaolin clay. XRD analysis, Figure 1 showed the disappearance of peaks at 2-theta 15.38, 17.86, 28.78, 47.56, 52.33, which represent the associated soluble metal ions as chlorides. The removal of these metal ions is already removed from kaolin clay as soluble metal ions. Figure 2 showed the XRD of kaolinite and iron hydroxides $Fe(OH)_3$ which compose $Fe(OH)_3$/kaolinite nanoplatelets.

FT-IR analysis

FT-IR analysis of the Jordanian kaolin clay, Figure 3 showed the hydroxyl stretching vibration bands at 3695, 3680 and 3622 cm^{-1}, which corresponds to the inner surface –OH stretching vibration of kaolinite. A band at 3483 cm^{-1} belongs to the stretching vibration of the outer-surface hydroxyl groups. The presence of ferric hydroxyl has a characteristic peak at 3456 cm^{-1}. The H-O-H bending of water is observed at band at 1651 cm^{-1} which is also assigned for the -OH bending vibration and C=O stretching vibration. The bands at 1116 cm^{-1} and 1045 cm^{-1} in the kaolin clay corresponding to Si-O-Si bending and Si-O is stretching vibrations. Absorption band at 914 cm^{-1} corresponds to the Al….O-H bending vibration. Bands at 540 and 470 cm^{-1} represent to Al-O-Si skeletal vibration.

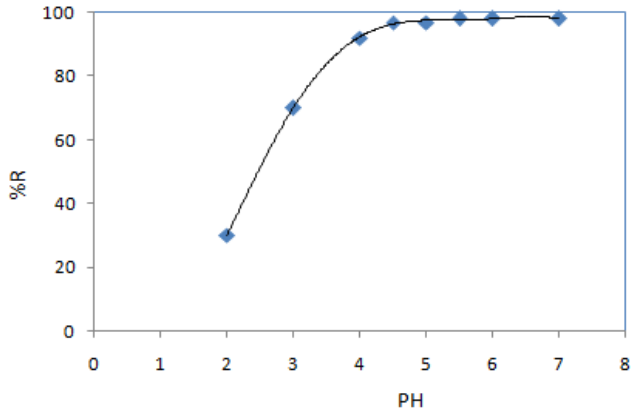

Fig. 8: Effect of PH on the percent removal of Pb(II) ion at 303 K

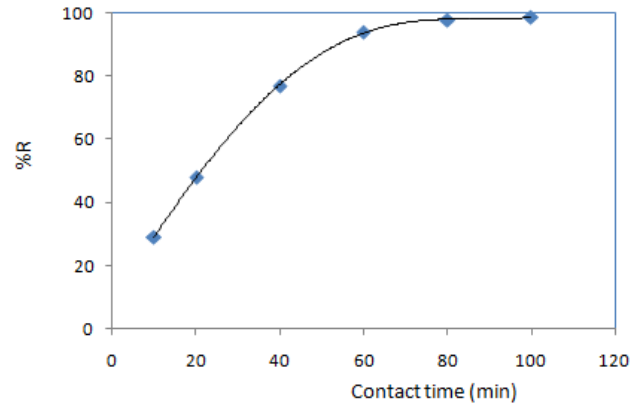

Fig. 9: Effect of contact time (min) on the percent removal of Pb(II ions from aqueous solution

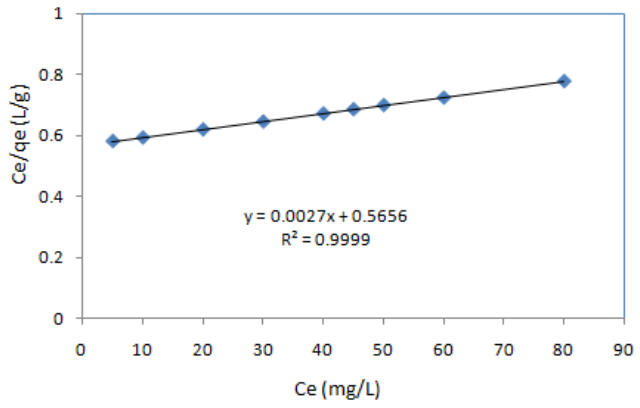

Fig. 10: Langmuir isotherms of Pb(II) ions onto $Fe(OH)_3$/ kaolinite nanoplatelets

The characteristic hydroxyl (-OH) bands of the prepared $Fe(OH)_3$/kaolinite nanoplatelets at 3699 cm^{-1}, 3657 cm^{-1} and 3626 cm^{-1} still exists (Fig. 4). These results indicated that the hydrogen bonding between the layers of raw kaolin and formation of new hydrogen bonding between the inner–surface hydroxyl groups. 516 cm^{-1} represent the Fe-O and Si-O-Al stretching. 475 cm^{-1} represent Si-O-Si bending. The obtained results indicated that the removal of associated metal oxides from the raw kaolin clay changed the structure to $Fe(OH)_3$/kaolinite nanoplatelets.

SEM and TEM analysis

Scanning electron microscopy image (SEM) of fine powder of raw Jordanian kaolin clay (Fig. 5). Particles of kaolin are plates in shape with size > 1µm. After treating raw kaolin clay with HCl and NaOH, $Fe(OH)_3$/kaolinite nanoplateles were obtained. Scanning electron microscopy analysis gave the nanoplateles obtained have size diameter ranging from 7.2-18.6 nm. TEM of the prepared $Fe(OH)_3$/kaolinite nanoplatelets. Figure 7 confirmed that nano $Fe(OH)_3$/kaolinite are in nanoplatelets.

Adsorption efficiency

Effect of pH

Effect of the solution pH on the adsorption process, experiments were carried out using 0.5g $Fe(OH)_3$/kaolinite nanoplatelets added to 100 ml of lead solutions with concentrations 10-100 mg/L, pH was adjusted in the range 1-6. By increasing the initial pH of the solution, the adsorption of Pb(II) ions increased. At low pH, a large number of H^+ compete with Pb(II) ions at the active sites of adsorbent, therefore the adsorption of Pb(II) ions decreased. By increasing the pH of the solution, the competition started decreasing, therefore the adsorption of Pb(II) increased sharply to approximately constant higher values of pH. The pH of the solution considerably affacted the adsorption and maximum removal was observed at pH 5.5 (Fig. 8).

Contact time

The effect of contact time on the adsorption of Pb(II) ions onto $Fe(OH)_3$/kaolinite nanoplatelets was investigated. The adsorption of Pb(II) ions increased considerably until the contact time 60 min. Effect of initial metal ion concentration Pb(II) ions adsorption by $Fe(OH)_3$/kaolinite nanoplatelets was studied in batch experiments using different initial Pb(II) concentrations of 5, 10, 20, 40, 60, 80 and 100 mg/L. The equilibrium uptake of the adsorbent was observed increasing gradually with an increasing initial concentration of Pb(II) ions. The increase of adsorption efficiency with the increase in Pb(II) ion concentration is probably due to higher interaction between the Pb(II) ions and sequestering sites present on the surface of the adsorbent (Fig. 9).

Effect of adsorbent dose

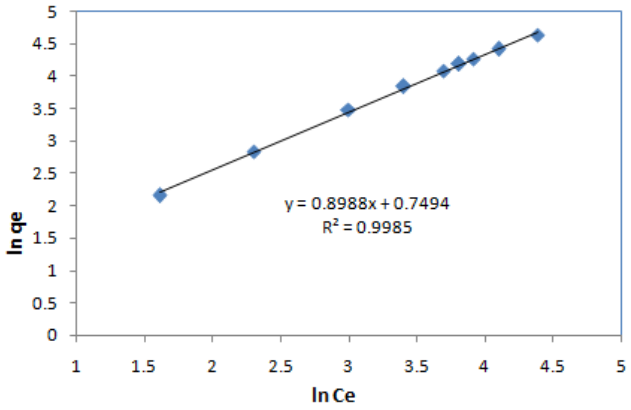

Fig. 11: Freundlich isotherms of Pb(II) ions onto $Fe(OH)_3$/kaolinite nanoplatelets

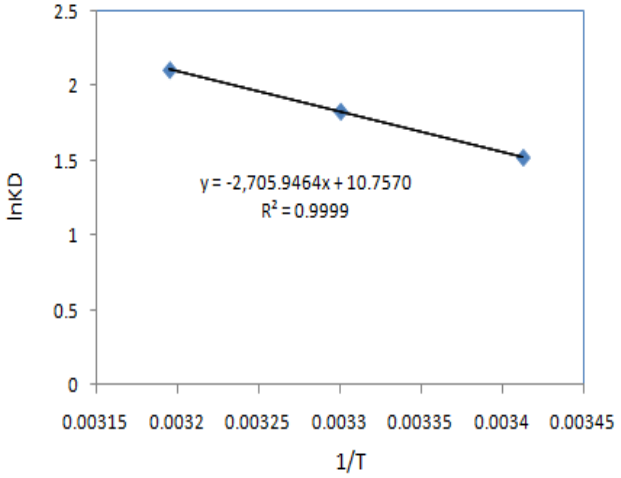

Fig. 12: Plot $\ln K_D$ versus 1/T for adsorption of Pb (II) ions onto $Fe(OH)_3$/kaolinite nanoplatelets

The adsorption efficiency for Pb(II) ions as a function of adsorbent was investigated. The percentage of the Pb(II) ions adsorption steeply increases with the adsorbent loading up to 1 g/0.1 L. This result can be explained by the fact that the adsorbent sites remain unsaturated during the adsorption reaction, whereas the number of sites available for adsorption site increases by increasing the adsorbent dose. The maximum adsorption of nano $Fe(OH_3$/kaolinite was attained at adsorbent dosage, 1g/0.1 L. Therefore, the optimum adsorbent dosage was taken as 0.5g/0.1L for further experiments. As the adsorbent dose increased, more active sites to bind Pb(II) ions, thus it results an increase in the adsorption efficiency until saturation.

Effect of temperature

The effect of temperature on the percent removal of Pb(II) ions from aqueous solutions by $Fe(OH)_3$/kaolinite nanoplatelets was 98.45-99.44% at temperatures 293, 303 and 313 K. From the obtained results that the percent removal at 303 and 313 K are very close.

Adsorption isotherms

Langmuir adsorption model was applied to the data by the following equation (Langmuir, 1918):

$$\frac{C_e}{q_e} = \frac{1}{q_m K_L} + \frac{1}{q_m} C_e \qquad (3)$$

Where q_m and K_L are the coefficients, q_e is the weight adsorbed per unit weight of adsorbent, and C_e is the pb(II) concentration in bulk solution at equilibrium. Equilibrium concentration C_e and equilibrium capacity q_e were calculated for each metal concentration. C_e was plotted against C_e/q_e and a straight line was fitted in the data (Fig 10). Correlation factor R^2 for, Pb(II) ions indicated that sorption followed Langmuir model. Values of Langmuir constants q_m and K_L were calculated from slope and intercept of line. For lead ions, R^2 values ≥ 0.9999, which clearly suggests the applicability of Langmuir adsorption model. The calculated constants q_m and K_L together with correlation coefficients (R^2) are given in Table 1. Low values of parameter, whereas K_L indicate that high affinity for Pb(II) ions.

Freundlich equation (Freundlich, 1906), also suggests that sorption energy exponentially decreases on completion of the sorption centers of an adsorbent. This isotherm is an empirical equation and can be employed to describe heterogeneous systems and is expressed as follows in linear form (Eq. 4).

$$\log q_e = \log K_F + \frac{1}{n} \log C_e \qquad (4)$$

Where K_F is Freundlich constant related to the bonding energy. 1/n is the heterogeneity factor and n (g/L) is a measure of the deviation from linearity of adsorption. Freundlich equilibrium constants were determined from the plot of $\ln q_e$ versus $\ln C_e$ (Fig. 11). The n value indicates the degree of non-linearity between solution concentration and adsorption as follows: if n = 1, then adsorption is linear; if n<1, then adsorption is a chemical process; if n >1, then adsorption is a physical process. The n value of Freundlich equation was found at 30 °C to be 1.133 for Pb(II) ions (Table 1). Since n lie between 1 and 10, this indicates the physical adsorption of Pb(II ions onto $Fe(OH)_3$/kaolinite nanoplatelets.

Thermodynamics study

The thermodynamic behavior of the adsorption of Pb (II), ions onto nano $Fe(OH)_3$/kaolinite prepared from Jordanian kaolin clay is reported. Thermodynamic parameters including the change in free energy (ΔG^o), enthalpy (ΔH^o) and entropy (ΔS^o) were calculated using Eq. 5.

Table 1: Langmuir and Freundlich isotherms for Pb(II) ions

Langmuir constants			Freundlich constants		
q_m	K_L	R^2	n	lnK_F	R^2
370.37	0.0048	0.9999	1.113	2.221	0.9985

Table 2: Thermodynamic parameters of Pb(II) ions

T/K	K_D	lnK_D	ΔG^o (kJ/mol)	ΔH^o (kJ/mol)	ΔS^o (J/K mol)
293	4.55	1.52	-3.702	22.489	89.434
303	6.35	1.83	-4.611		
313	8.02	2.11	-5.491		

Table 3: Comparison of $Fe(OH)_3$/kaolinite nanoplatelets with other adsorbents

Adsorbents	q_e (mg/g)	References
Rice husk	10..8	Feng et al. (2004)
Penut husk powder	19.7	Abdelfattah et al. (2016)
Maize cob	21.4	Muthusamy & Murugan (2016)
Modified loqual leaves	29.6	Awwad & Salem (2012)
Ficus benghalensis L	28.6	Surisetty e al. (2013)
Palm shell axctivated carbon	95.2	Issabayeva et al. (2006)
coconut shell activated carbon	92.4	Caccin et al. (2016)
A native natural bentonite	8.5	Esmaeili & Eslami (2019)
NanoIllite/smectiteClay	0.3	Yin et al. (2018)
natural sepiolite	93.4	Bektaş et al. (2004)
Mercapto Sepiolite	97	Liang et al. (2013)
Nano-clay adsorbent	56.2	Unuabonah et al. (2008)
Surface modification of kaolinite	53.3	Al-Harahsheha et al. (2009)
Unmodified kaolinite clay	16.4	Unuabonah et al. (2007)
Phosphate-modified kaolinite clay	17.9	Unuabonah et al.(2007)
Modified kaolinite clay with Al sulfate	20	Jiang et al. (2009)
Unmodified kaolinite clay	125	Ogbu et al. (2019)
Modified sawdust clay	142.8	Ogbu et al. (2019)
Kaolinite/smectite natural composite	517.3	El-Nagger et al. (2019)
Natural mixture of kaolinite-albite	24.1	Eba et al. (2011)
Montmorillonite-illite clay	25.6	Eba et al. (2011)
Iron oxide/hydroxide nanoparticles	527.94	Rahimi et al. (2015)
mesoporous magnetite nanospheres	19	Kumari et al. (2015)
Magnetite Loaded on silica Support	25.3	Mahmoud et al. (2019)
$Fe(OH)_3$/kaolinite nanolatelets	370.7	Present work

$$\Delta G = RTlnK_d \quad (5)$$

Where, R is the universal gas constant (8.314 J/mol K). T (K) is the temperature. K_D is the distribution coefficient. The thermodynamic equilibrium constant (K_D) of the adsorption is defined as shown in Eq. 6.

$$K_D = \frac{C_a}{C_e} \quad (6)$$

Where, C_a is mg of adsorbate adsorbed per liter and C_e is the equilibrium concentration of solution, mg/L. According to thermodynamics, the Gibb's free energy change is also related to the enthalpy change (ΔH^o) and entropy change (ΔS^o) at constant temperature by the Gibbs–Helmholtz relation (Eqs. 7-8).

$$\Delta G^o = \Delta H^o - T\Delta S^o \quad (7)$$

$$\ln K_D = \frac{\Delta H^o}{RT} - \frac{\Delta S^o}{R} \quad (8)$$

According to Eq. 8, the values of enthalpy change (ΔH^o) and entropy change (ΔS^o) were calculated from the slope and intercept of the plot of ln K_D vs. 1/T (Fig. 12). The calculated values of thermodynamic parameters ΔG^o, ΔH^o and ΔS^o for the adsorption of Pb(II) onto $Fe(OH)_3$/kaolinite nanoplatelets are reported in Table 2. A negative value of the free energy (ΔG^o) indicated the spontaneous nature of the adsorption process. It was also noted that the change in free energy, increases with rise in temperature. This could be possibly because of activation of more sites on the surface of nanoplatelets $Fe(OH)_3$/kaolinite with increase in temperature or that the energy of adsorption sites has an exponential distribution and a higher temperature enables the energy barrier of adsorption to be overcome. For physical adsorption, the free energy change (ΔG^o) ranges from (-20 to 0) kJ/ mol and for chemical adsorption it ranges between (-80 and -400) kJ/mol. The ΔG^o for Pb(II) adsorption onto nanoplatelets $Fe(OH)_3$/kaolinite was in the range of (-3.7 to -5.5) kJ/ mol and so the adsorption was predominantly physical adsorption. A positive value of ΔS^o as 89.434 J/ mol K showed increased randomness at solid solution interface during the adsorption of Pb(II) ions onto nanoplatelets $Fe(OH)_3$/kaolinite.

Comparison of $Fe(OH)_3$/kaolinite nanoplatelets with other adsorbents

A comparative of the maximum adsorption capacity, q_{max} of $Fe(OH)_3$/kaolinite nanoplatelets with some other adsorbents reported in literature is given in Table 3. Differences in q_{max} are due to the nature and properties of each adsorbent such as surface area and the main functional groups in the structure of the adsorbent. A comparison with other adsorbents indicated a high Pb(II) ions adsorption capacity of $Fe(OH)_3$/kaolinite nanoplatelets.

CONCLUSIONS

The $Fe(OH)_3$/kaolinite nanoplatelets prepared from the Jordanian kaolin clay deposits, Jordan could be used as potential adsorbent for the removal of Pb(II) ions from aqueous solutions. The batch adsorption parameters: pH of solution, adsorption dose, contact time, initial Pb(II) concentration and temperature were found to be effective on the adsorption process. Thermodynamic parameters ΔG^o, ΔH^o and ΔS^o showed the endothermic and spontaneous nature of the adsorption of Pb(II) ions onto $Fe(OH)_3$/kaolinite nanoplatelets. Langmuir model showed the best fit for the experimental data. The maximum adsorption capacity of Pb(II) ions onto platelets $Fe(OH)_3$/kaolinite nanoplatelets at pH 6.0–7.0 and 30°C is 370.37mg/g. Compared to various adsorbents reported in the literature, $Fe(OH)_3$/kaolinite nanoplatelets showed good promise for its use in water and wastewater treatment.

ACKNOWLEDGEMENTS

Authors are thankful for the Royal Scientific Society and the University of Jordan, Jordan for providing the necessary facilities to carry out this work.

REFERENCES

Abdelfattah, I., Ismail, A.A., Al Sayed, F., Almedolab, A., 2016. Biosorption of heavy metal ions in real industrial wastewaterusing peanut husk as efficient and cost effective adsorbent. Environmental Nanotechnology, Monitoring & Management 6, 176-183.

Al-Harahsheh, M., Shawabkeh, R., Al-Harahsheh, A., Tarawneh K., 2009. Surface modification and characterization of Jordanian kaolinite: Application for lead removal from aqueous solutions. Applied Surface Science 255, 8098-8103.

Al-Jlil, S.A., Alsewailem, F., 2009. Saudi Arabian clays for lead removal in wastewater. Applied Clay Science, 2009, 42, 671-674.

Al-Shannag, M., Al-Qodah, Z., BaniMelhem, K., Qtaishat, M.R., Alkasrawi, M., 2015. Heavy metal ions removal from metal plating wastewater using electrocoagulation: Kinetic study and process performance. Chemical Engineering Journal 260, 749-56.

Amer, M.W., Kahlili, F. I., Awwad, A.M., 2010. Adsorption of lead, zinc and cadmium ions on polyphosphate-modified modified kaolinite clay. Journal of Environmental Chemistry and Ecotoxicology 2, 1-8.

Anitha, K., Namsani, S., Singh, J.K., 2015. Removal of heavy metal ions using a functionalized single-walled carbon nanotube: a molecular dynamics study. The Journal of Physical Chemistry A 119, 8349-8358.

Awwad, A.M., Salem, N.M., 2012. Biosorption of copper(II) and lead(II) ions from aqueous solutions by modified

loquat (*Eriobotrya japonica*) leaves (MLL). Journal of Chemical Engineering and Materials Science 3, 7-17.

Bankole, M.T., Abdulkareem. A.S., Mohammed, I.A., Ochigbo, S.S., Tijani, J.O., Abubakre, O.K., Roos, W.D., 2019. Selected heavy metals removal from electroplating wastewater by purified and polyhydroxylbutyrate functionalized carbon nanotubes adsorbents. Scientific Reports 9, 4475.

Basu, M., Guha, A.K., Ray, L., 2015. Biosorptive removal of lead by lentil husk. Journal of Environmental Chemical Engineering 3, 1088-1095.

Bektaş, N., Ağım, A.B., Kara., S., 2004. Kinetic and equilibrium studies in removing lead ions from aqueous solutions by natural sepiolite. Journal of Hazardous Materials 112, 115-122.

Bilgin, M., Tulun, S., 2015. Use of diatomite for the removal of lead ions from water: thermodynamics and kinetics. Biotechnology & Biotechnological Equipment 29, 696-704.

Caccin, M., Giorgi, M., Giacobbo, F., Ros, M.D., 2016. Besozzi, L., Mariani, M. Removal of lead (II) from aqueous solutions by adsorption onto activated carbons prepared from coconut shell. Desalination and Water Treatment 57, 4557-4575,

Chukwuemeka-Okorie, H.O., Ekemezie, P.N. Akpomie, K.G. Olikagu, C.S., 2018. Calcined corncob-kaolinite combo as new sorbent for sequestration of toxic metal ions from polluted aqua media and desorption. Frontiers in Chemistry 6, 1-12.

Eba, F., Ondo, J.A., Gueu, S., Nlo, J.N., 2011. Biboutou, R.K. Content by using natural mixture of kaolinite-albite-montmorillonite-illite clay. Journal of Applied Sciences 11, 2536-2545.

Eiband, M.M.S.G., Trindade, K.C., Gama, A., de Melo, J.V. Martínez-Huitle, C.A., Ferro, S., 2014. Elimination of Pb^{+2} through electrocoagulation: Applicability of adsorptive stripping voltammetry for monitoring the lead concentration during its elimination. Journal of Electroanalytical Chemistry 717-718, 213-218.

El-Naggar, I.M., Ahmed, S.A., Shehata, N. A., 2019. novel approach for the removal of lead(II) ion from wastewater using Kaolinite/Smectite natural composite adsorbent. Applied Water Science 9, 7.

El Sayed, E., 2018. Natural diatomite as an effective adsorbent for heavy metals in water and wastewater treatment (a batch study). Water Science 32, 32-43.

El-Shahat, M.F., Shehata, A.M.A., 2013. Adsorption of lead, cadmium and zinc ions from industrial wastewater by using raw clay and broken clay-brick waste. Asian Journal of Chemistry 25, 4284-4288.

Erdem, E., Karapinar, N., Donat, R., 2004. The removal of heavy metal cations by natural zeolites. Journal of Colloid and Interface Science 280, 309-314.

Esmaeili, A., Eslami, H., 2019. Efficient removal of Pb*(II)* and Zn*(II)* ions from aqueous solutions by adsorption onto a native natural bentonite. MethodsX 6, 1979-1985.

Etoh, M.A., Dina, D., 2015. Ngomo, H.M.; Ketcha, J.M. Adsorption of Pb^{2+} ions onto two clays: Smectite and kaolin the role of their textural and some physicochemical properties. International Journal of Applied Research 1, 793-803.

Feng, Q., Lin, Q., Gong, F., Sugita, S., Shoya, M., 2004. Adsorption of lead and mercury by rice husk ash. Journal of Colloid and Interface Science 278, 1-8.

Fiol, N., Villaescusa, I., Martínez, M., Miralles, N., Poch, Serarols, J., 2006. Sorption of Pb(II), Ni(II), Cu(II) and Cd(II) from aqueous solution by olive stone waste. Separation and Purification Technology 50, 132-140.

Freundlich, H.M.F., 1906. Über die adsorption in lösungen. Zeitschrift für Physikalische Chemie 57, 385-470.

Golkhah, S., Mousavi, H. Z., Shirkhanloo, H., Khaligh, A., 2017. Removal of Pb(II) and Cu(II) ions from aqueous solutions by cadmium sulfide nanoparticles. International Journal of Nanoscience and Nanotechnology 13, 105-117.

Gupta, V.K., Agarwal, S., Saleh, T.A., 2011. Synthesis and characterization of alumina-coated carbon nanotubes and their application for lead removal. Journal of Hazardous Materials 185, 17-23.

Hadavifar, M., Bahramifar, N., Younesi, H., Li. Q., 2014. Adsorption of mercury ions from synthetic and real wastewater aqueous solution by functionalized multi-walled carbon nanotube with both amino and thiolated groups. Chemical Engineering Journal 237, 217-228.

Hamadneh, I., Abu-Zurayk, R., Abu-Irmaileh, B., Bozeya, A., 2015. Adsorption of Pb(II) on raw and organically modified Jordanian bentonite. Clay Minerals 50, 485-496.

Huang, Z-H., Zheng, X., Lv, W., Wang, M., Yang, Q-H., Kang, F., 2011. Adsorption of lead(II) ions from aqueous solution on low-temperature exfoliated graphene nanosheets. Langmuir 27, 7558-7562.

Ibrahim, M.N.M., Ngah, W.S.W., Salleh, N.M., Hashim, R. A., 2010. Novel agricultural waste adsorbent for the removal of lead(II) ions from aqueous solutions. Journal of Hazardous Materials 182, 377-385.

Issabayeva, G., Aroua, M.K., Sulaiman, N.M.N., 2006. Removal of lead from aqueous solutions on palm shell activated carbon. Bioresource Technology 97, 2350-1235.

Jiang, M.Q., Wang, Q.P., Jin, X.Y., Chen, Z.L., 2009. Removal of Pb(II) from aqueous solution using modified and unmodified kaolinite clay. Journal of Hazardous Materials 170, 332-339.

Jiang, M.Q., Jin, X.Y., Lu, X.Q., Chen, Z.L., 2010. Adsorption of Pb(II), Cd(II), Ni(II) and Cu(II) onto natural kaolinite clay. Desalination 252, 33-39.

Kavak, D., 2013. Removal of lead from aqueous solutions by precipitation: statistical analysis and modeling. Desalination and Water Treatment 51, 1720-1726.

Kul, A.R., Koyuncu, H., 2010. Adsorption of Pb(II) ions from aqueous solution by native and activated bentonite: kinetic, equilibrium and thermodynamic study. Journal of Hazardous Materials 179, 332-339.

Kumar, S., Nair, R.R., Pillai, P.B., Gupta, S. N., Iyengar, M.A.R., Sood, A.,K., 2014. Graphene oxide-$MnFe_2O_4$ magnetic

nanohybrids for efficient removal of lead and arsenic from water. ACS Applied Materials and Interfaces 6, 17426-17436.

Kumari, M., Pittman, Jr., C.U., Mohan, D., 2015. Heavy metals chromium (VI) and lead (II)] removal from water using mesoporous magnetite (Fe_3O_4) nanospheres, Journal of Colloid and Interface Science 442, 120-132.

Langmuir, I., 1918. The adsorption of gases on plane surfaces of glass, mica and platinum. Journal of the American Chemical Society 40, 1361-1403.

Li, Y-H., Ding, J., Luan, Z., Di, Z., Zhu, Y., Xu, C., Wu, D., Wei, B., 2003. Competitive adsorption of Pb^{2+}, Cu^{2+} and Cd^{2+} ions from aqueous solutions by multiwalled carbon nanotubes. Carbon 41, 2787-2792.

Li, Y-H., Wang, S., Wei, J., Zhang, X., Xu, C., Luan, Z., Wu, D., Wei, B., 2002. Lead adsorption on carbon nanotubes. Chemical Physics Letters 357, 263-266.

Liang, S., Ye, N., Hu, Y., Shi, Y., Zhang, W., Yu, W., Wu, X., Yang, J., 2016. Lead adsorption from aqueous solutions by a granular adsorbent prepared from phoenix tree leaves. RSC Advances 6, 25393.

Lin, L., Xu, X.; Papelis, C., Cath, T. Y., Xu, P., 2014. Sorption of metals and metalloids from reverse osmosis concentrate drinking water treatment solids. Separation and Purification Technology 134, 37-45.

Mahmoud, A.S., Youssef, N., Osama, A.M., Selim, M., 2019. Removal of Lead Ions from Industrial Wastewater Using Magnetite Loaded on Silica Support. Egyption Journal of Chemistry 62, 2163-2173.

Mansoorian, H.J., Mahvi, A.H., Jafari, A.J., 201. Removal of lead and zinc from battery industry wastewater using electrocoagulation process: Influence of direct and alternating current by using iron and stainless steel rod electrodes. Separation and Purification Technology 135, 165-175.

Mengistie, A.A., Rao, S., Rao, A.V.P., 2008. Singanan, M. Removal of lead (II) ions from aqueous solutions using activated carbon from Militia ferruginea plant leaves. Bulletin of the Chemical Society of Ethiopia 22, 349-360.

Momčilović, M., Purenović, M., Bojić, A., Zarubica, A., Ranđelović, M., 2011. Removal of lead(II) ions from aqueous solutions by adsorption onto pine cone activated carbon. Desalination 2011, 276, 53-59.

Mousa, S.M., Ammar, N.S., Ibrahim, H.A., 2016. Removal of lead ions using hydroxyapatite nano-material prepared from phosphogypsum wast. Journal of Saudi Chemical Society 20, 357-365.

Munagapati, V.S., Yarramuthi, V., Nadavala, S.K., Alla, S.R., Abburi, K., 2010. Biosorption of Cu(II), Cd(II) and Pb(II) by *Acacia leucocephala* bark powder: Kinetics, equilibrium and thermodynamics. Chemical Engineering Journal 157, 357-365.

Muthusamy, P., Murugan, S., 2016. Removal of lead ion using maize cob as a bioadsorbent. International Journal of Engineering Research and Application 6, 5-10.

Ogbu, I.C., Akpomie, K.G.,. Osunkunle, A.A., Eze, S.I., 2019. Sawdust-kaolinite composite as efficient sorbent for heavy metal ions. Bangladesh Journal of Scientific and Industrial Research 54, 99-110.

Omar, W., Al-Itawi, H., 2007. Removal of Pb^{2+} ions from aqueous solutions by adsorption on kaolinite clay. American Journal of Applied Sciences 4, 502-507.

Pang, F.M., Kumar, P., Teng, T.T., Omar, A.K.M., Wasewar, K.L., 2011. Removal of lead, Zinc and iron by coagulation-flocculation. Journal of Taiwan institute of chemical Engineers 42, 809-815.

Poursani, A.S., Hassani, A., Shariat, S.M., Nouri, J., 2016. The Synthesis of nano TiO_2 and Its use for removal of lead ions from aqueous solution. Journal of Water Resource and Protection 2016, 8, 438-448.

Rahimi, S., Moattari, R.M., Rajabi, L., Derakhshan, A.A., Keyhani, M., 2015. Iron oxide/hydroxide (α,γ-FeOOH) nanoparticles as high potential adsorbents for lead removal from polluted aquatic media. Journal of Industrial and Engineering Chemistry 23, 33-43.

Reátegui-Romero, W., Cadenas-Vásquez W. j., María E., King-Santos, M.E., Alvarez, W.F.Z., Posadas, R.A.Y., 2019. Evaluation of Pb (II) adsorption from aqueous solutions using *Brassica nigra* as a biosorbent, The Open Biotechnology Journal 13, 77-92.

Reddy, D.H.K., Seshaiah, K., Reddy, A.V.R., Rao, M.M., Wang, M.C., 2010. Biosorption of Pb^{2+} from Aqueous Solutions by *Moringa oleifera* bark: Equilibrium and Kinetic Studies. Journal of Hazardous Materials 174, 831-838.

Safatian, F., Doago, Z., Torabbeigi, M., Shams, H. R., Ahadi, N., 2019. Lead ion removal from water by hydroxyapatite nanostructures synthesized from egg sells with microwave irradiation. Applied Water Science 9, 108.

Salihi, I.U., Kutty, S.R.M., Isa, M.H., 2017. Adsorption of lead ions onto activated carbon derived from sugarcane baggase, IOP conference: Materials Science and Engineering 201, 012034.

Salem, N.M., Awwad, A.M., Al-Dujaili,A.H., 2012. Biosorption of Pb(II), Zn(II), and Cd(II) from aqueous solutions by (Eriobotrya japonica) loquat bark. International Journal of Environmental Protection 2, 1-7.

Sangeetha, K., Vidhya, G., Vasugi, G., Girija, E.K., 2018. Lead and cadmium removal from single and binary metal ion solution by novel hydroxyapatite/alginate/gelatin nanocomposites. Journal of Environmental Chemical Engineering 6, 1118-1126.

Sari, A., Tuzen, M., Citak, D., Soylak, M., 2007. Equilibrium, kinetic and thermodynamic studies of adsorption of Pb(II) from aqueous solution onto Turkish kaolinite clay. Journal of Hazardous Materials 149, 283-289.

Sarkar, Z.K., Sarkar, F.K., 2013. Selective removal of lead (II) ion from wastewater using superparamagnetic monodispersed iron oxide (Fe_3O_4) nanoparticles as a effective adsorbent. International Journal of Nanoscience and Nanotechnology 9, 109-114.

Soltani, R.D.C., Khorramabadi, G.S., Khataee, A.R., Jorfi, S., 2014. Silica nanopowders/alginate composite for adsorption of lead(II) ions in aqueous solutions, Journal

of the Taiwan Institute of Chemical Engineers 45, 973-980.

Surisetty, V.R., Kozinski, J., Nageswara, L.R., 2013. Biosorption of lead ions from aqueous solution using *Ficus benghalensis* L. Journal of Engineering 2013, 1-8.

Tasar, S., Ozar, A., 2020. A Thermodynamic and kinetic evaluation of the adsorption of Pb(II) Ions using peanut (*Arachis Hypogaea*) shell-based biochar from aqueous media. Polish Journal of Environmental Studies 29, 293–305.

Unuabonah, F.I., Olu-Owolabi, B.I., Adebowale, K.O., 2016. Compative adsorption of metal ions onto goethite-humic acid- modified kaolinite clay, International Journal of Environmental Science Technology 13, 1043-1054.

Unuabonah, E.I., Adebowale, K.O., Olu-Owolabi, B.I., 2007. Kinetic and thermodynamic studiesof the adsorption of lead (II) ions onto phosphated-modified kaolinite clay. Journal of Hazardous Materials 144, 386-395.

USEPA (United States Environmental Protection Agency)., 2019. https://www.epa.gov/

Wang, X., Guo, Y., Yang, L., Han, M., Zhao, J., 2012. Nanomaterials as sorbents to remove heavy metal ions in wastewater treatment. Journal of Environmental and Analytical Toxicology 2, 154.

Wang, H.J., Zhou, A.L., Peng, F., Yu, H., Chen, L.F., 2007. Adsorption characteristic of acidified carbon nanotubes for heavy metal Pb(II) in aqueous solution. Materials Science and Engineering: A 466, 201-206.

Wang, S-G., Gong, W-X., Liu, X-W., Yao, Y-W., Gao, B-Y., Yue, Q-Y., 2007. Removal of lead(II) from aqueous solution by adsorption onto manganese oxide-coated carbon nanotubes. Separation and Purification Technology 58, 17-23.

Wang, X.S., Lu, H.J., Zhu,L., Liu, F., Ren, J., 2010. Adsorption of Lead(II) Ions onto magnetite nanoparticles. Adsorption Science and Technology 28, 407-417.

WHO., 1984. guideline values for drinking water quality. Vol. 1, Recommendations. World Health Organization: Geneva, 1, 81.

Yang, J., Hou, B., Wang, J., Tian, B., Bi, J., Wang, N., Li, X.; Huang, X., 2019. Nanomaterials for the removal of heavy metals from wastewater. Nanomaterials 9, 424.

Yarkandi, N.H., 2014. Removal of lead (II) from waste water by adsorption. International Journal of Current Microbiology and Applied Sciences 3, 207-228.

Yin, J., Deng, C., Yu, Z., Wang, X., Xu, G., 2018. Effective removal of lead ions from aqueous solution using nanoIllite/smectite clay: misotherm, kinetic and thermodynamic modelling of adsorption. Water 10, 210.

Yusoff, S., Kamari, A., Putra, W., Ishak, C., Mohamed, A., Hashim, N., Isa, I., 2014. Removal of Cu(II), Pb(II) and Zn(II) ions from aqueous solutions using selected agricultural wastes: adsorption and characterisation studies. Journal of Environmental Protection 5, 289-300.

Zhao, G., Ren, X., Gao, X., Tan, X., Li, J., Chen, C., Huang, Y., Wang, X., 2011. Removal of Pb(II) ions from aqueous solutions on few-layered graphene oxide nanosheets. Dalton Transactions 40, 10945-10952.

Visit us at: http://bosaljournals.com/chemint/
Submissions are accepted at: editorci@bosaljournals.com